EXTENDED TISSERAND-POINCARÉ GRAPH AND MULTIPLE LUNAR SWINGBY DESIGN WITH SUN PERTURBATION

Daniel García Yárnoz, Chit Hong Yam, Stefano Campagnola, Yasuhiro Kawakatsu

ISAS/JAXA, Department of Space Flight Systems

ABSTRACT

This paper presents a systematic approach to generate first guesses of multiple lunar swing-by sequences for interplanetary small satellite missions. The Sun third body perturbation plays an important role essentially providing free Δv between lunar swing-bys. As a first approach, an extension of the classical Tisserand-Poincaré graph is presented, in which the potential gains by solar perturbation between flybys can be estimated. Secondly, following an approach proposed by Lantoine & McElrath [1], a database of Moon-to-Moon transfers is generated with a continuation method. New families with multiple revolutions and families close to libration point orbits are generated. The database can be accessed and transfers retrieved to quickly generate sequences in similar fashion to a Lambert problem solver. Two practical examples are presented: a transfer to the Earth-Moon L_2 point, and an escape strategy for the DESTINY mission to initiate the transfer to asteroid Phaeton.

Index Terms— Lunar swing-bys, Tisserand-Poincaré graph, Sun's third body pertubation, DESTINY, EQUULEUS

1. INTRODUCTION

New trends in miniaturisation and advances in CubeSat-size subsystems are enabling small missions beyond low Earth orbit. Due to cost contraints, however, such missions would rarely afford a dedicated launch or direct insertion into their desired transfer orbits. Fortunately, the characteristics of the Earth-Moon system with a single massive moon allow for flexible and relatively simple trajectory designs with lunar swing-bys to circunvent problems such as low initial orbital energy or incorrent phasing in the case of piggy-back launches. The use of a multiple lunar swing-by sequence to pump up the hyperbolic escape velocity of interplanetary transfers or to design libration point escape or insertion trajectories has been proposed in literature [1, 2, 3] and is a well-known strategy demonstrated in various missions [4, 5].

Currently, JAXA is considering similar strategies for two of their future missions. The technology demonstrator mission DESTINY [6], with its new main mission objective to reach comet Phaethon [7], plans to make use of a multiple lunar swing-by sequence to obtain the required escape velocity after a spiraling phase from its launcher injection orbit. On an unrelated programme, NASA is offering CubeSat launch opportunities in Moon-bound orbits on the first test launch of their SLS [8], and JAXA is proposing among other applications a small mission to the Earth–Moon L_2 region after a series of lunar swing-bys. The Earth–Moon phases of these two missions have two intrinsically different objectives: a high escape velocity with respect to the Moon, or a transfer at low velocities to a Moon libration orbit, but both would benefit from a sequence of lunar flybys.

One of the key desired aspects of this type of trajectories is the exploitation of the Sun third body perturbation, as it was done in Lunar-A and Planet-B [9]. This perturbation plays a critical role to change the two-body energy of the spacecraft between lunar flybys. As reported widely in literature (see for example [4]), the net effect of the third body perturbation in orbits on the same plane as the perturbing body is a deceleration or pericentre lowering for orbits with apocentre in the first and third quadrants when plotted on a synodic rotating frame (with the perturbing body, in this case the Sun, assumed on the negative X–axis), and an acceleration or pericentre raising for orbits with the apocentre on the second and fourth quadrants, assuming prograde orbits. This is illustrated in Fig. 1 for example orbits of interest for the DESTINY mission. These perturbed orbits are useful between two consecutive lunar encounters, and may be exploited for tuning the phasing, increasing or decreasing the hyperbolic escape velocity with respect to the Moon and ultimately the Earth–Moon system, or achieving the correct escape direction [1].

Example trajectories have been proposed for JAXA's missions, but given the large number of possible combinations, a more systematic search may be required in certain cases, to guarantee that most sequences of interest have been considered.

2. DYNAMICAL MODEL

In order to systematically generate a variety of first guesses for a sequence of lunar gravity assists, a simplified Circular Restricted Three Body Problem (CR3BP) for the Sun-Earth system is assumed. The equations of motion in the synodic frame, centred in the barycentre, with the positive X–axis to-

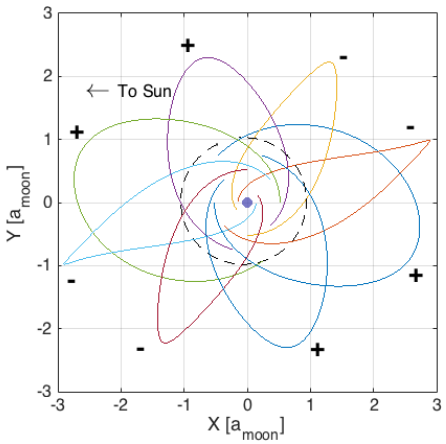

Fig. 1. Orbit evolution with solar perturbation for orbits with apogee at two Moon semi-major axis and perigee at 200 000 km. Plus and minus markers indicate the apocentre variation direction.

wards the Earth are given by:

$$\begin{aligned}
\ddot{x} &= 2\dot{y}+x-\frac{(1-\mu)x_1}{r_1^3}-\frac{\mu x_2}{r_2^3} \\
\ddot{y} &= -2\dot{x}+y-\frac{(1-\mu)y_1}{r_1^3}-\frac{\mu y_2}{r_2^3} \\
\ddot{z} &= -\frac{(1-\mu)z_1}{r_1^3}-\frac{\mu z_2}{r_2^3}
\end{aligned} \tag{1}$$

where distances have been normalized by one astronomical unit AU (Earth at $1-\mu$, with μ the gravitational parameter ratio of the Sun–Earth system $\mu = \mu_2/(\mu_1+\mu_2)$), and times have been normalized with the inverse of the frequency of rotation of the synodic frame ($\Omega = \sqrt{(\mu_1+\mu_2)/AU^3}$). Positions without subscript are with respect to the barycentre, while the subscripts 1 and 2 indicate position with respect to the primary and the secondary (Sun and Earth in this case), see Fig. 2 for a schematic of the reference frame.

The Moon is assumed in a circular orbit around the Sun coplanar with the Sun and Earth, and its gravity is not considered between lunar encounters. This assumption allows to generate transfers independent of the Earth's position along its orbit (repeting every synodic month), but the validity of the sequences in a full model could be put into question. However, it has been demonstrated that sequences generated with equivalent models are surprisingly good initial guesses for a full model propagation [1].

Trajectories are propagated with an Adam-Bashford variable step ode solver implemented in the DEPAC package [10]. Althought the dynamics presented are three-dimensional, this work limits itself to planar trajectories in the hypothetical plane of the three massive bodies Sun, Earth and Moon, leaving out pi transfers and other out of plane resonances.

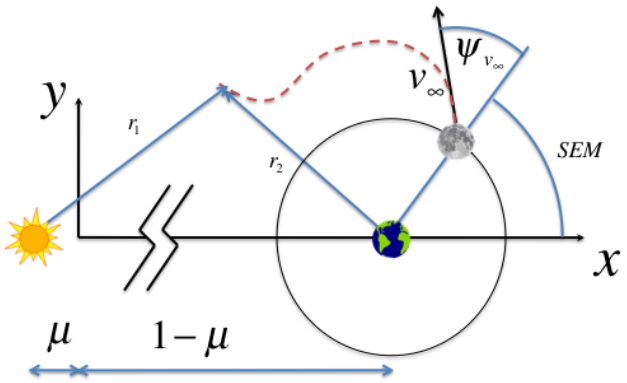

Fig. 2. Synodic frame and initial variables definition.

3. EXTENDING THE TISSERAND-POINCARÉ GRAPH

A useful tool to design multiple-gravity assists trajectories is the Tisserand-Poincaré (T–P) graph. Without delving into the details (for a more detailed explanation, see [11, 12]), Figure 3 represents the Tisserand-Poincaré graph of the Earth–Moon systen in apocentre–pericentre, with distances normalized by the Moon's semimajor axis a_M. It is important to note that Tisserand parameter (T_M) level sets are used instead of v_∞ level sets, with T_M given as:

$$T_M = \frac{2a_M}{r_a+r_p} + 2\sqrt{\frac{2r_a r_p}{(r_a+r_p)a_M}} = 3 - v_\infty^2 \approx J \tag{2}$$

This allows the graph to extend beyond the patched conic allowed region (shaded rectangular area with $r_p < 1$ and $r_a > 1$), and makes it possible to plot level curves at the Tisserand parameter (a good approximation of the Jacobi constant J) of the various Lagrangian points of the Earth–Moon system. This is relevant to study the potential of some trajectories to transfer to libration point orbits.

The graph illustrates an example sequence of flybys along a constant line of T_M or v_∞, including a v_∞-leveraging technique (VILT) maneuver raising the pericentre in order to reach a line of lower v_∞. When introducing the Sun's third body perturbation it is possible to receive a free boost or "Sun-kick" between flybys depending on the relative geometry. It is possible to show that these Sun-kicks are provided closely following lines of slope -1.

In order to study analytically this effect in a first order approximation, we resort to the variational equations of motion in true anomaly, as reported in [13]:

$$\begin{aligned}
\frac{da}{d\nu} &= \frac{2pr^2}{\mu_2(1-e^2)^2}\{e\sin(\omega_p+\nu)F_R + \frac{p}{r}F_T\} \\
\frac{de}{d\nu} &= \frac{r^2}{\mu_2}\{\sin(\omega_p+\nu)F_R + (1+\frac{r}{p})\cos(\omega_p+\nu)F_T + e\frac{r}{p}F_N\}
\end{aligned} \tag{3}$$

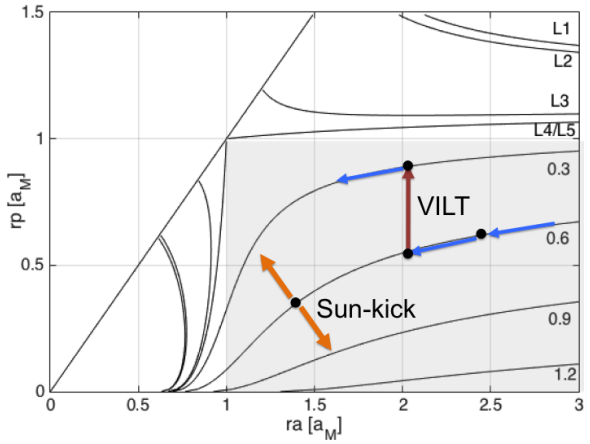

Fig. 3. Tisserand-Poitcaré graph with level sets for v_∞ v_∞ values from 0.3 to 1.2 km/s, and the libration points. The effect of a VILT maneouver and a "Sun-kick" is indicated.

where a, e, ω_p, ν are the initial orbital elements of a spacecraft orbit around the Earth; inclination and right ascension are assumed zero in this planar approximation.

Taking into account $p = a(1-e^2)$ and $r = p/(1+e\cos\nu)$, and substituting the third body attraction of the Sun as the perturbing force, it is possible to integrate in true anomaly over one revolution from pericentre to pericentre (from 0 to 2π) to obtain first-order relations identical, save nomenclature differences, to the ones already calculated in [14]:

$$\begin{aligned} \Delta a &\approx 0 \\ \Delta e &= \frac{15\pi}{2\mu} a^3 e\sqrt{1-e^2}\sin 2(\omega_p - \theta) \end{aligned} \tag{4}$$

where the angle θ represents half the rotation of the apsis line in the synodic frame along the orbit, given by $\theta = \pi\sqrt{a^3/\mu}$, and all variables are normalized. The term $\omega_p - \theta$ can be considered as an average argument of pericentre, or its value at apocentre. The values obtained represent the variation over one revolution for orbits such as the ones plotted in Fig. 1.

The first relation (constant semi-major axis over one revolution) already hints at the Sun-kick acting on the T–P graph along lines of slope -1 ($\Delta r_p = -\Delta r_a$), while the second relation, with its sinusoidal term of two times the average argument of pericentre, explains the behaviour in the various quadrants advanced in the introductory section.

The maximum deviations in eccentricity for a given orbit, which in turn provide the maximum displacements in the T–P graph, corrrespond to the sine term equal to ± 1. However, the integration of the equations of perturbation theory has been performed assuming constant orbital elements over one revolution, or small variations with respect to a non-perturbed trajectory. This is not completely applicable in the case at hand, as the perturbation is large and the orbital elements deviate far from the original values. To obtain the achievable maximum deviation, each point in the level sets is propagated for a full orbit and a small optimisation is run with the initial argument of pericentre as optimisation variable. Fig. 4 plots the maximum deviations in the level set lines predicted by the analytical approximation, compared with the results of the optimisation.

Selected points in the original level sets are marked with circles, while the displaced points are indicated with triangular markers (pointing up for pericentre raising and down for lowering).

It can be observed that the analytical approximation provides a conservative estimate of the expected maximum deviations. An exception to this is the case for hyperbolic escape velocity of 1.2 km/s, where the analytical formula provides unfeasible results with negative pericentre radius. Per definition, the analytical results follow lines of constant semi-major axis (markers along lines of slope -1), while the numerical propagated results have larger deviations and do not follow that pattern for high apocentres and hyperbolic excess velocity.

All the points provided by the analytical formula (save again the unfeasible case of negative pericentres) are reachable with the numerical propagation. It is thus a good conservative estimate that can be calculated at a mere fraction of the computing time required for optimising.

For apocentre heights above 1.2 Moon semi-major axis, the effect of the Sun-kicks becomes increasingly important, and above $2a_M$ it can easily substitute particular VILT maneuvers if the geometric configuration is appropriate. The graph also shows that the Earth–Moon libration point regions, or at least their required energies, can be reached with aid from the Sun, in particular for hyperbolic excess velocities around 0.3 km/s and apocentre heights above $2a_M$.

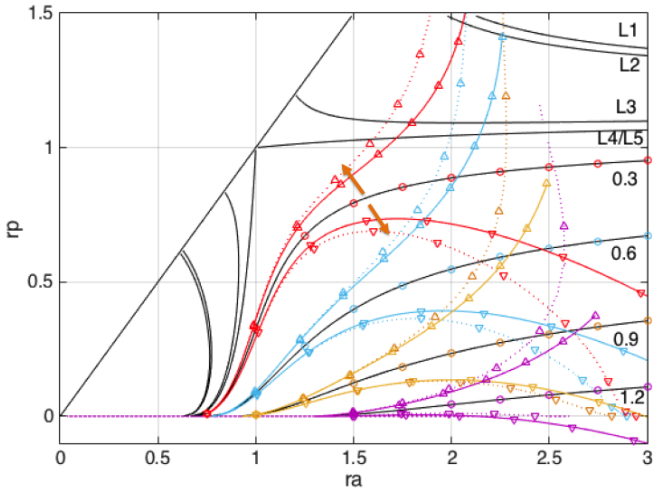

Fig. 4. Maximum achievable deviation on the T–P graph due to a "Sun-kick", with an analytical approximation (continuos lines) and the propagated and optimised results (dashed).

4. MOON TO MOON TRANSFER DATABASE

The Tisserand-Poincaré graph is useful to determine the potential reachable regions with a Sun-kick from a given orbit. However, the extent and even the direction of the kick are highly dependant on the relative geometry of the orbit with respect to the Sun direction. Furthermore, multiple revolutions before Moon encounters could add up to the total effect, or they could counteract partly or totally each other.

Unlike in the traditional Lambert problem, there's no closed analytical solution for Moon-to-Moon (or point-to-point) transfers in the CR3BP. In order to generate sequences of such transfers, Lantoine & McElrath [1] proposed storing a database of Moon-to-Moon legs for quick access with any of the traditional swing-by sequence generation methods. The Earth–Moon system is particularly suited for that purpose, given that it comprises a single massive moon. This work extends the previous analysis with new families of transfers, as well as including multiple spacecraft revolutions.

The departure conditions of a Moon-to-Moon leg can be established with just 3 variables: the angles between the anti-solar direction, Earth and the Moon at the initial time SEM, the modulus of the hyperbolic escape excess velocity with respect to the Moon v_∞, and the latitude angle of this hyperbolic escape velocity Ψ_{v_∞}, which is defined as the angle between the radial direction Earth–Moon and the hyperbolic escape excess velocity (see Fig. 2 for a graphical representation of these variables). With these parameters, the initial conditions in an inertial reference frame centred at the Earth and with axis parallel to the synodic frame at the initial time are given by:

$$r_I = \begin{bmatrix} a_M \cos SEM \\ a_M \sin SEM \\ 0 \\ -v_M \sin SEM + v_\infty \cos\left(SEM + \Psi_{v_\infty}\right) \\ -v_M \cos SEM + v_\infty \sin\left(SEM + \Psi_{v_\infty}\right) \\ 0 \end{bmatrix} \tag{5}$$

with $v_M = \sqrt{\mu/a_M}$ being the Moon's circular orbital velocity. Once transformed into the synodic frame, the initial conditions are propagated with the dynamics in Eq. **??**. The only additional fourth variable that unequivocally defines a transfer is the transfer time t_F, forming the problem variable vector $\lambda = \left[SEM, v_\infty, \Psi_{v_\infty}, t_F\right]$.

In addition, the Jacobian of the equations of motion is given by:

$$J_{CR3BP} = \begin{bmatrix} [0] & I_3 \\ [J_{21}] & \begin{bmatrix} 0 & 2 & 0 \\ -2 & 0 & 0 \\ 0 & 0 & 0 \end{bmatrix} \end{bmatrix} \tag{6}$$

with

$$J_{21} = \begin{bmatrix} 1 & 0 & 0 \\ 0 & 1 & 0 \\ 0 & 0 & 0 \end{bmatrix} - (1-\mu)\left(\frac{I_3}{{r_1}^3} - 3\frac{r_1 {r_1}^T}{{r_1}^5}\right) - \mu\left(\frac{I_3}{{r_2}^3} - 3\frac{r_2 {r_2}^T}{{r_2}^5}\right) \tag{7}$$

The Jacobian is integrated along with the state vector to obtain the state transition matrix at each point. The state transition matrix is used to calculate derivatives of the final error with respect to each variable in vector λ.

In order to generate the full database of trajectories, a scan is performed in $\lambda_{i,i=1,2}$, with the SEM angle varying from 0 to $2pi$ in steps of $pi/144$, and the v_∞ ranging from 0.3 to 2 km/s in steps of 0.1 km/s. This range was limited in the lower side due to the patched conics approximation at the Moon becoming less accurate, and on the upper side given that escape velocities of the Earth–Moon system close to 3 km/s can already be achieved.

The unknown variables $\lambda_{j,j=3,4}$ are optimised for each case of λ_i, with cost function the final position error with respect to the Moon:

$$\epsilon = (x_{If} - x_{Mf})^2 + (y_{If} - y_{Mf})^2 \tag{8}$$

For each converged solution, the partial derviatives of the final error with repect to each initial variable ϵ_λ are calculated. Once a preliminary grid search finds a solution, that family can be extended using a simple continuation method in both $\lambda_{i,i=1,2}$, where the guesses for the unknown variables are generated with:

$$\lambda_j(\lambda_i + \delta\lambda_i) = \lambda_j(\lambda_i) - \frac{\epsilon_{\lambda_i}}{\epsilon_{\lambda_j}}\delta\lambda_i \tag{9}$$

Solutions are stored with the four variables defining the transfer λ_i, and in addition the final SEM, v_∞ and Ψ_{v_∞} to be able to look up and connect subsequent legs, and the minimum radius to Earth during transfers r_{2min}.

For comparison reasons with the work in [1], families are stored into 4 categories: outgoing-outgoing (*oo*), outgoing-incoming (*oi*), incoming-incoming (*ii*) and incoming-outgoing (*io*). The type of transfer is easily identified as a funcion of Ψ_{v_∞}, as for outgoing trajectories $\cos(\Psi_{v_\infty}) > 0$ at start and/or end (and conversely < 0 for incoming ones). Families are further categorized as a function of the "approximate" number of spacecraft revolutions n_{SC}, and the "approximate" number of Moon revolutions n_M.The use of the apelative "approximate" will become clear in the following discussion.

Figure 5 plots the families for one of the cases presented by Lantoine & McElrath with $v_\infty = 1.2$ km/s and n_{SC} =1. A set of additional subfamilies appear for high number of revolutions of the Moon, with energies similar to L_1 and L_2, that was only present in the above reference for $n_M = 4$. As they already pointed out, due to the symmetries of the problem (although not exactly symmetric in the y-axis, as evidenced by the different energies for L_1 and L_2), families appear to repeat after a rotation of pi in SEM angle.

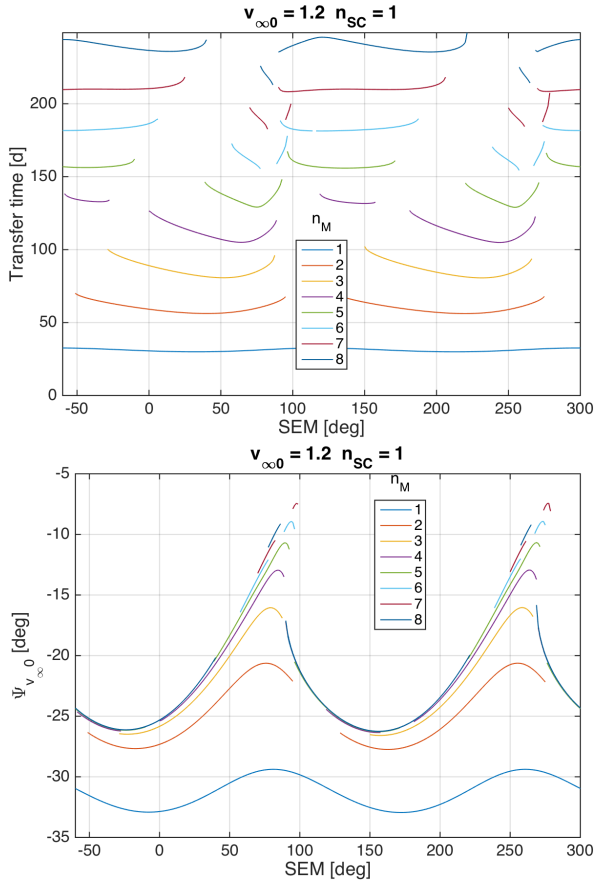

Fig. 5. Families of outgoing-incoming transfers for $v_\infty = 1.2$ km/s and $n_{SC} = 1$, transfer time (top) and initial Ψ_{v_∞} (bottom).

Taking advantage of this, families are extended by backward and forward continuation, and when available using the quasi-symmetric transfers as initial guess for the optimisation. In subsequent plots, only half of the circunference of SEM angle will be represented.

4.1. Families topology

The proposed classification faces a series of challenges. When the Sun perturbation is neglected, each of the families corresponds to a resonant transfer of the type n_{SC}:n_M, or its variants n_{SC}:n_M^- and n_{SC}:n_M^+. However, with third body perturbation, families are highly dependant on the relative geometry, they break into sub-families, and reconnect with other sub-families of different category and number of revolutions (usually on a fold in SEM, when they become tangent to the Moon's orbit).

This is shown in Fig. 6-top, which plots half the map of a set of *oi* and *oo* families. Except for the self-contained *1:1* resonances, and the *1:2 oo* case, for longer transfer times subfamilies connect in loops or in a helix fashion. The duration is sometimes no longer in accordance with the resonance they originated from: there are *1:5* transfers with longer duration than some *1:6* ones for example, and thus the numbering is ony indicative of the approximate number of revolutions. Given that the Sun perturbation changes some prograde trajectories into retrograde, or that trajectories passing near the libration point often have additional apocentres and pericentres, the number of spacecraft revolutions is not strict as well. The naming has been kept though for consistency with families at lower or higher v_∞. Similar structures are found in cases with more spacecraft revolutions (see Fig. 6-bottom).

It is also possible to observe sections of the same family that overlap in SEM angle (most clear for family with n_M=6 or 7 in Fig. 5). This adds difficulty to the design of methods using the database. The suitability of the SEM angle for parameterizing the families, particularly near the folds where the derivatives become infinite, can be questioned. The transfer time is still a useful variable for discriminating between families, but the hyperbolic escape velocity latitude presents problems as well, with families close together for long transfer times.

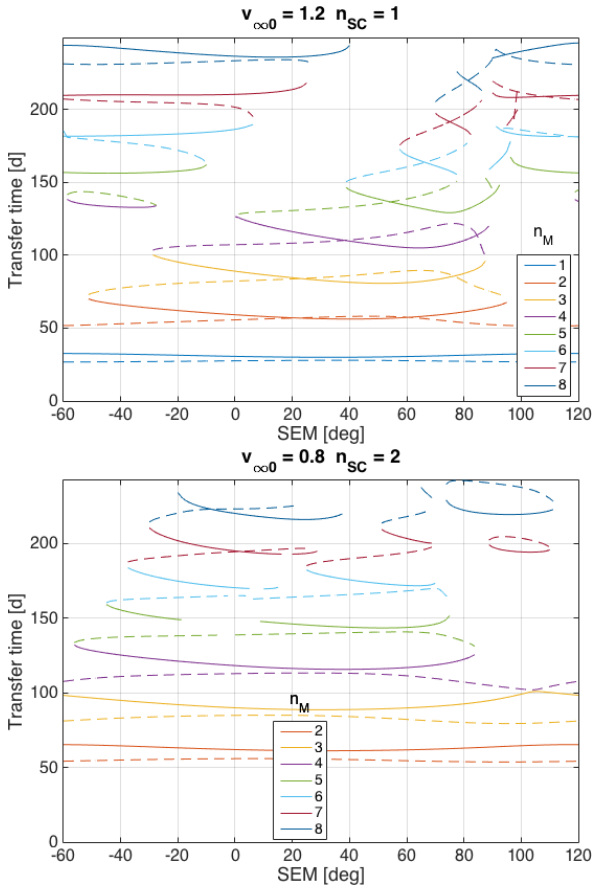

Fig. 6. Transfer times for outgoing-incoming (continuous) and outgoing-outgoing (dashed) transfers for v_∞=1.2 km/s and n_{SC}=1 (top), and v_∞=0.8 km/s and n_{SC}=2 (bottom).

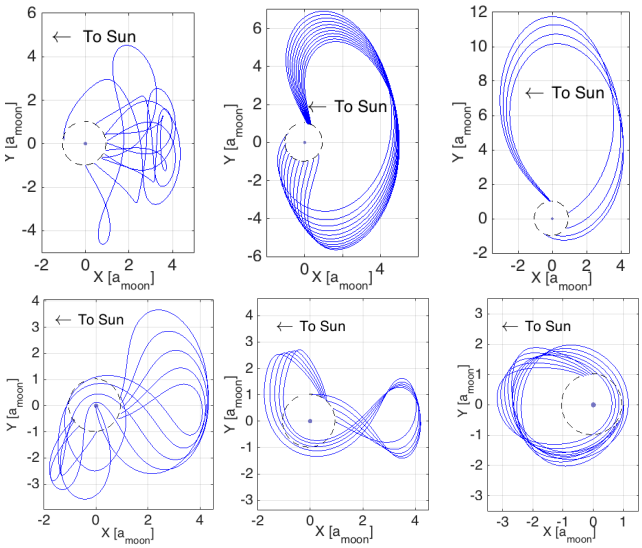

Fig. 7. Example *oi 1:7* trajectories with v_∞=1.2 km/s (top) and *oi 2:7* with v_∞=0.8 km/s

The transfers of each subfamily have very diverse and distict shapes when represented in the synodic frame. To illustrate this, Fig. 7 presents example *oi* trajectories for each of three sub-families that appear with n_M=7 (solid dark red lines in Fig. 6), with one (top) and two (bottom) spacecraft revolutions. Several of the transfers shadow some of the well-know families of the CR3BP. Top middle transfers shadow planar Lyapunov or Strömgren's *a* class orbits [15], while the top and bottom right transfers are close to different sections of Strömgren's *g-g'* class orbits, the second one also sometimes refered to as Distant Prograde Orbits (DPOs).

The incoming-outgoing case includes a special type of transfer: if less than one revolution is allowed, it results in very fast retrograde transfers that only exist for high hyperbolic escape velocities (over 2 km/s, an example is plotted in Fig. 8) and are hardly affected by the Sun.

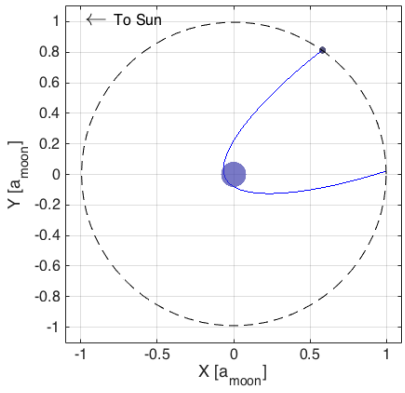

Fig. 8. Incoming-outgoing retrograde trajectory example with v_∞=2 km/s.

5. APPLICATION EXAMPLES

This section presents two application examples to construct Moon-to-Moon transfers using the above generated database.

5.1. EQUULEUS

In 2015 NASA issued an annoucement of opportunity for CubeSats to cislunar space as secondary payloads to be launched along their Exploration Mission-1 (EM-1) [8]. JAXA proposed a 6U CubeSat candidate mission to the Earth–Moon L_2 region: EQUULEUS (EQUilibriUm Lunar-Earth point 6U Spacecraft), which made it into the downselection process. Its main objectives are to study the Earth–Moon plasmasphere and demonstrate trajectory navigation and control in the Weak Stability Boundary region.

Launch conditions are selected for the main EM-1 mission targeting the Moon, with several options that are expected to change during the mission design process. In addition, a full launch window would imply a variety of dates and conditions at the encounter with the Moon. This makes it a perfect candidate to demonstrate the flexibility of the database to quickly generate guesses for a variety of initial conditions.

One such set of initial conditions currently under study, including ephemeris time and hyperbolic incoming escape velocity at the Moon in Ecliptic 2000 are given by:

$$\begin{aligned} et &= 566901751.54244 \ \ s \\ v_\infty &= [-0.6874 \ \ -0.3746 \ \ -0.1658] \ \ km/s \end{aligned} \tag{10}$$

which translates into SEM=186.38679 deg and v_∞=0.8 km/s.

The final target orbit of EQUULUS is a halo orbit around the Earth–Moon L_2. This implies lowering the hyperbolic incoming escape velocity at the Moon as much as possible. As shown in section 3, it is possible to easily reach the L_2 region energies when considering the Sun third body perturbation from v_∞ around 0.3 km/s, or even 0.6 km/s if the apocentre radius is high enough.

In order to systematically study available transfers, we set up a simple branch and pruning algorithm, recursively adding legs from the above presented initial conditions to a final Moon encounter with v_∞ lower than 450 m/s in less than 1 year. The pruning of unfeasible branches is performed:

- When the final v_∞ of a branch is above 2 km/s (contrained by the current range covered by the database),
- When the minimum radius from Earth during a leg r_{2min} is below 10 000 km, to discard trajectories close to collisions with the secondary
- When the patched conics swing-by results in a pericentre radius at the Moon lower than $r_{p_{min}}$=200 km.

This condition can be expressed in the problem's parameters, with μ_M the gravittional constant of the Moon, as:

$$\Delta\Psi_{v_\infty} - \leq \pi - 2\arccos\frac{1}{1 + r_{p_{min}}{v_\infty}^2/\mu_M} \tag{11}$$

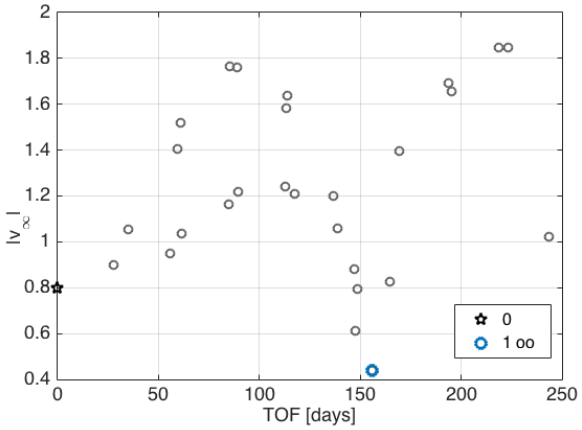

(a) One leg

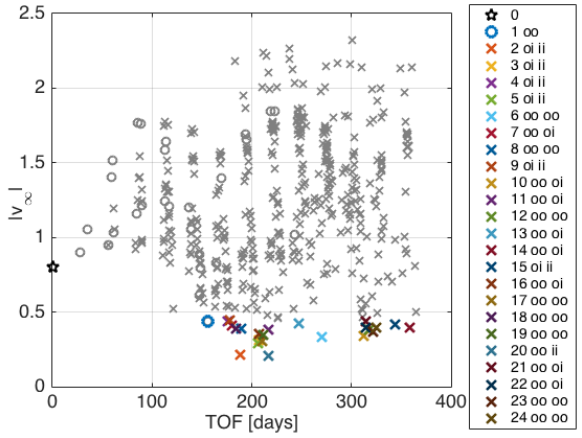

(b) Two legs

Fig. 9. Available transfers to the Moon.

A one leg scan of the database already provides a set of 25 feasible transfers. Out of them, one outgoing-outgoing transfer meets the requirements of final hyperbolic escape velocity at the Moon, with a duration of sightly above 150 days, as shown in Fig. 9a (colored marker).

For each of the one leg transfers, the branch and pruning continues with a second leg, increasing the number of available options to 469 (including the previous 25), and a total of 24 of them meeting the requirements, some with final v_∞ as low as 200 m/s, see Fig. 9b. Fig. 10 shows a few selected transfers: the top left figure presents the only single leg trasnfer meeting the constraints, along all two-legged transfers with final v_∞ under 300 m/s. There is a diversity in the type of transfers and the shape of the trajectories. As expected, the lowest v_∞ are obtained with transfers almost tangent to the Moon's orbit, which as explained in Section 4.1, correspond to the hinges between family types. The bottom left trajectory for example has two legs with two spacecraft revolutions, although in the second one the trajectory does not cross the orbit of the Moon before the final time. The bottom right trajectory on the other hand uses the *1:5* single leg transfer in the upper left to insert into a *1:2 ii* leg after a very low altitude flyby (just 289 km above the lunar suface) which causes the sharp turn in direction at the swing-by. Given the low altitude of the flyby, a re-optimisation in the full model may prove unfeasible.

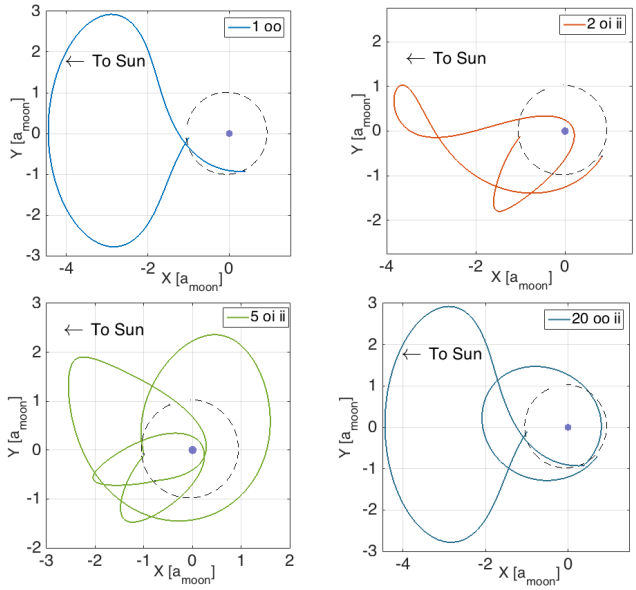

Fig. 10. Selected transfers to the Moon.

The process can be iteratively repeated for any number of legs until the maximum time allows.

5.2. DESTINY mission to asteroid Phaethon

The case of the DESTINY spacecraft [7] is the diametrally oposed problem: instead of decreasing the v_∞, we are interested in increasing it as much as possible to escape the Earth–Moon system at higher velocities; and instead of knowing the initial conditions, it is part of the final conditions that are given, namely a date and a v_∞ vector with respect to the Earth. In the current baseline, the escape from the Earth system is constrained to be 1.5 km/s. From the hyperbolic escape velocity relation:

$$v_2{}^2 = 2\mu/r_2 + v_\infty{}^2 \tag{12}$$

we obtain that, for that v_∞, the velocity with respect to the Earth at Moon distance, in inertial frame, is equal to 2.08 km/s. Given the Moon's orbital velocity, this translates into a lunar swing-by v_∞ ranging from approximately 1.1 km/s to 3.1 km/s.

For a particular case of the interplanetary trajectory (see [7] for the various options), the velocity at escape from the Earth system in Ecliptic 2000 is:

$$v_{\infty E} = [-1.3453 \;\; 0.6633 \;\; -0.0014] \;\; km/s \tag{13}$$

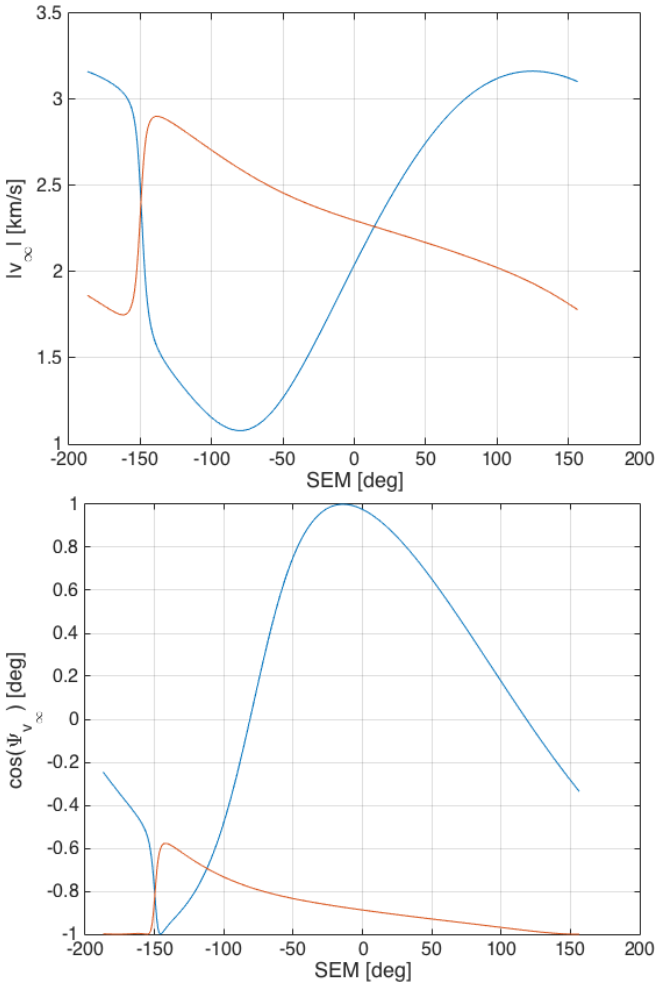

Fig. 11. Hyperbolic escape velocity and cosine of the latitude angle at the Moon.

Propagating backwards, and neglecting the out-of-plane component at the Moon, two sets of possible lunar encounters prior to the escape date are plotted in Fig. 11, using the method described in [16].

The range of v_∞ corresponds to the expected values, with a clear minimum close to $SEM = -90°$. As expected, this takes place when the outgoing v_∞ at the flyby is aligned with the Moon velocity, and thus $\cos(\Psi_{v_\infty}) \approx 0$. To have a most efficient swing-by sequence for escape, the last Moon encounter should be sought near this region, preferably although not required with increasing v_∞ at each encounter.

Without further information on the initial conditions at the moment, other than the fact that it is a spiriling up phase, the lower the v_∞ at the previous flyby, the better. The extended T–P graph showed that the velocities required could be achieved from an encounter with v_∞ as low as 0.3 km/s provided that the apocenter radius was large enough. Figure 12 plots the final conditions for particular sets of *oo*, *oi* and *ii* families for this velocity, overlaying the outgoing required conditions to escape the Earth in the correct direction. It is possible to pinpoint several intersections that meet the constraints in SEM and v_∞. However, they may not be feasible in terms of the patched conics allowed rotation of the v_∞ (calculated with Eq. 11).

In order to systematically search for feasible solutions,a scan of the database is performed to detect all possible transfers that meet the following criteria:

- Final conditions of the branch (SEM and v_∞) matching the required outgoing conditions in Fig. 11,
- Initial $v_{\infty 0} \leq$ 0.6 km/s, as the sequence sought is one of increasing v_∞ from the spiriling phase,
- Final $v_{\infty f} \leq$ 2 km/s (this essentially limits the lunar swing-by to be in the region of -150$\leq SEM_f \leq$0 from Fig. 11-top),
- Minimum radius from Earth $r_{2min} \geq$ 10 000 km
- Patched conics allowed rotation resultings in a pericentre radius at the Moon higher than $r_{p_{min}}$=200 km.

Fig. 13 plots the resulting trajectories from this scan. It shows that there is a range of transfer shapes and types already at low velocities that can be patched with the escape hyperbola. Given that the database contains only transfers at fixed steps of v_∞, in reality a continuum of transfers for all intermediate v_∞ would be obtained in most of the cases. None of the trajectories, save maybe one in the top-left figure (*oo* with v_∞ = 0.3 km/s) takes place particularly close to the absolute minimum in Fig. 11. However, they do not deviate far from it.

The same procedure can be recursively applied backwards, to add additional legs to the trajectory in order to match and phase with any launch or spiriling initial conditions.

6. DISCUSSION AND CONCLUSIONS

A systematic approach to generate multiple lunar swing-by sequences has been proposed and demonstrated. This is a useful tool considering the increase in small interplanetary satellite missions that will require one or more lunar swing-bys to achieve the required escape conditions. Exploiting the Sun third body perturbation, which provides a "Sun-kick" to the spacecraft equivalent to a free Δv, the energy of the spacecraft can be increased or decreased to meet the desired target conditions.

An extension of the Tisserand-Pointaré graph is presented that allows a first estimate of the potential of these Sun-kicks. Furthermore a database of Moon-to-Moon transfers has been generated in the Sun–Earth Circular Restricted Three Body Problem, considering the Moon only for connecting legs of

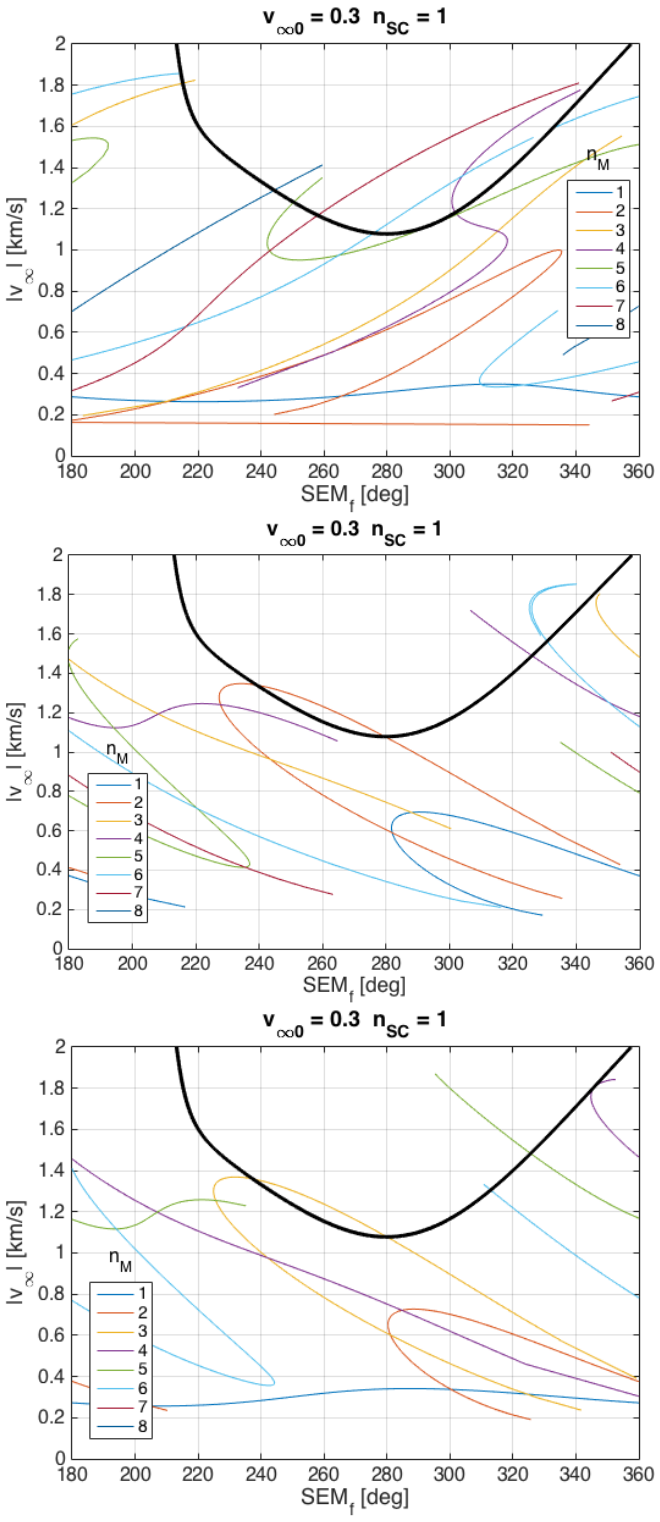

Fig. 12. Final v_∞ versus final SEM angle for *oo*, *oi* and *ii* families. Required escape conditions are overlayed in black.

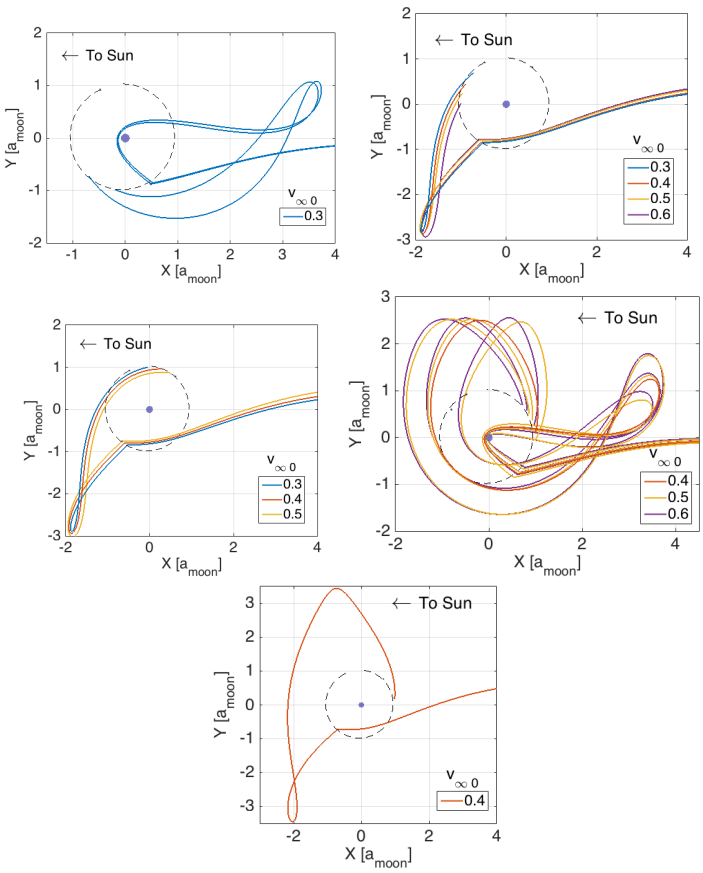

Fig. 13. Options for last leg of DESTINY before escape. Families *oo*, *oi* and *ii*, including the possibility of multiple spacecraft revolutions can be found.

the trajectory in a patched conics approximation. For simplicity and to allow a partially epoch-free generation of solutions, all transfers are considered planar with the Moon in a circular orbit around the Earth also on the ecliptic plane. The database extends the work of [1] to new families of transfers close to the L_1 and L_2 energies, and to multiple spacecraft revolutions.

Finally, the database is used to design trajectories for two practical examples: a CubeSat mission to the Earth–Moon L_2 point, and DESTINY's escape sequence into its interplanetary transfer to asteroid Phaethon. Simple branch and pruning methods are applied to quickly generate initial guesses for further optimisation in a full model. A wide range of solutions can be generared for both problems and are presented in this work.

There are nonetheless several limitations to the use of the models presented, associated with some of the simplyfying assumptions, and regarding the completeness of the scans performed in this fashion. The CR3BP is a good approximation for feasibility studies and to generate initial guesses. However, a full model propagation and reoptimisation of the trajectories is required to take into account effects such as the inclination and eccentricity of the Moon's orbit, or the eccentricity of the Earth. In particular, families of Moon-to-Moon

transfers close to the L_1 and L_2 energies may vary significantly or even dissappear for certain conditions. Furthermore, out-of-plane transfers, such as the well-known π-transfers, are currently not considered, and they would add additional flexibility to the design process.

This work is currently an ongoing project and further extensions are foreseen. In particular, a regularization of the equations of motion would allow for more robust continuation methods to generate and extend the database, to avoid problems at collisions with the secondary (the Earth). These trajectories may be of little practical use, but for the sake of completeness they should be included in the database. Secondly, the continuation method can be further improved with a pseudo-arclength continuation, in order to continue the families beyond folds. Currently, a change of family type usually takes place at each fold (e.g. from *oo* to *oi* when the trajectory is tangent to the Moon's orbit), but different classification and storage of the families can be devised to unify families that reconnect or separate families that branch off.

All in all, the approach presented has proven to be effective and allows to have a quick grasp of the dynamics of the problem and a detailed analysis of the solution options.

7. ACKNOWLEDGEMENTS

The work presented in this paper was funded by the Japan Society for the Promotion of Science (JSPS) Fellowship for Overseas Researchers.

8. REFERENCES

[1] G. Lantoine and T. P. McElrath, "Families of Solar-perturbed Moon-to-Moon transfers," in *24th AAS/AIAA Spaceflight Mechanics Meeting*. AAS/AIAA, 2014, AAS 14-471.

[2] Timothy P. McElrath, "Using gravity assists in the Earth–Moon system as a gateway to the Solar System," in *Global Space Exploration Conference*, 2012, GLEX–2012.05.5.2x12358.

[3] Hongru Chen, Yasuhiro Kawakatsu, and Toshiya Hanada, "Earth escape from a Sun–Earth halo orbit using unstable manifolds and lunar gravity assists," in *25 th Workshop on Astrodynamics and Flight Mechanics*. ISAS/JAXA, 2015.

[4] Junichiro Kawaguchi, Hiroshi Yamanaka, Tono Uesugi, and Hiroki Matsuo, "On making use of lunar and solar gravity assist in Lunar-A, Planet-B missions," *Acta Astronautica*, vol. 35, no. 9–11, pp. 633–642, 1995.

[5] David W. Dunham, José J. Guzmán, and Peter J. Sharer, "STEREO trajectory and maneuver design," *Johns Hopkins APL Technical Digest*, vol. 28, no. 1, pp. 104–125, 2009.

[6] Y. Kawakatsu, K. Nishiyama, I. Funaki, and T. Iwata, "DESTINY mission description and its value," in *Proceedings of 29th International Symposium on Space Technology and Science*, 2013, 2013–k–47.

[7] Bruno Victorino Sarli, Chit Hong Yam, Y. Kawakatsu, and Makoto Horikawa, "Low-thrust trajectory design for the DESTINY mission to (3200) Phaeton," in *26th Space Flights Mechanics Meeting*, 2016, AAS 16–387.

[8] NASA, "Space Launch Systems (SLS) Scoundary Payload User's Guide," Tech. Rep. SLS-SPIE-HDBK-005, NASA, 2015.

[9] K. Yagasaki, "Sun-perturbed Earth-to-Moon transfers with low energy and moderate flight time," *Celestial Mechanics and Dynamical Astronomy*, vol. 90, pp. 197–212, 2004.

[10] Lawrence F. Shampine and H. A. Watts, *DEPAC: Design of a User Oriented Package of ODE Solvers*, Sandia National Laboratories. UC 32. Volume 79-2374 of Sandia report, 1979.

[11] S. Campagnola and R. P. Russell, "Endgame problem part 1: V-infinity leveraging technique and the leveraging graph," *Journal of Guidance, Control, and Dynamics*, vol. 33, no. 2, pp. 463–475, 2009.

[12] S. Campagnola and R. P. Russell, "Endgame problem part 2: Multibody technique and the Tisserand–Poincaré graph," *Journal of Guidance, Control, and Dynamics*, vol. 33, no. 2, pp. 476–486, 2009.

[13] P. W. Fortescue, J. P. W. Stark, and G. G. Swinerd, Eds., *Spacecraft Systems Engineering*, pp. 93–96, John Wiley & Sons Ltd., Chichester, UK, third edition, 2003.

[14] G. E. Cook, "Luni-Solar perturbations of the orbit of an Earth satellite," *The Geophysical Journal of the Royal Astronomical Society*, vol. 6, no. 3, pp. 271–291, 1962.

[15] R.A. Broucke, "Periodic orbits in the restricted three-body problem with Earth–Moon masses," Tech. Rep. 32-1168, JPL, Pasadena, Jet Propulsion Laboratory, California Institute of Technology, 1968.

[16] Chit Hong Yam, *Design of Missions to the Outer Planets and Optimization of Low-Thrust, Gravity Assist Trajectories via Reduced Parameterization*, pp. 96–105, Ph.D. thesis. Purdue University, May 2008.